Review

Israel Journal of Chemistry

doi.org/10.1002/ijch.202100049

Chiral Resolution via Cocrystallization with Inorganic Salts

Oleksii Shemchuk,[b] Fabrizia Grepioni,[a] Tom Leyssens,[b] and Dario Braga*[a]

Abstract: The coordination mode to lithium, magnesium, calcium and zinc cations of racemic vs. enantiopure amino acids and racetam APIs is analysed and its effect on chiral selection critically reviewed. It is shown that chiral resolution in the solid state can be obtained via cocrystallization of racemic compounds with an achiral inorganic salt coformer, such as LiX (X = Cl, Br, I) or $ZnCl_2$, which favour tetrahedral coordination in the solid state. The chiral selection may take the form of conglomerate crystal formation or of selective homochiral aggregation in racemic crystals. When cocrystallization involves alkaline earth metal cations, such as Ca^{2+} and Mg^{2+}, which favour octahedral coordination, heterochiral complexation is observed in most cases, with formation of racemic crystals.

Keywords: Chiral resolution · amino acids · racetams · lithium · zinc

1. Introduction

Chirality of chemical substances is ubiquitous in nature. The essential building blocks of life are made up of chiral units characterized by unique homochiralities (proteins built of L-amino acids, RNA and DNA composed of D-sugars).[1] In living organisms only one of the two enantiomers of a chiral compound can be found. Therefore, organisms that consume a chiral compound in the form of a racemate usually metabolize only one of its enantiomers. Metabolic and regulatory processes mediated by biological systems are sensitive to stereochemistry, exhibiting different reactions upon interaction with a pair of enantiomers.[2] Metabolic processes, enzymatic reactions and messenger-receptor interactions are examples of the reactions susceptible to enantioselectivity.[3] Thus, stereochemistry must be taken into account in the development of novel xenobiotics (e.g. pharmaceuticals, nutraceuticals, agrochemicals and fragrances), and it is of paramount importance in the pharmaceutical industry where, to date, approximately 50% of the marketed drug compounds contain a chiral centre essential to their functioning.[4] A pair of enantiomers of a chiral biologically active compound typically have different pharmacological activities, metabolic effects, metabolic rates and toxicities, due to the high degree of stereoselectivity of enzymatic reactions and other biological processes.[5] Where one enantiomer exhibits the desired pharmacological activity, the other might have no or a much weaker effect as well as side effects or even toxicity (Thalidomide being a well-known example[6]).[7] Nevertheless, a large number of chiral drugs has been historically administered as racemates.[8] Nowadays, regulatory authorities require independent pharmacological tests for each enantiomer as well as their combined effects, and only the therapeutically active isomer should be used in a marketed drug product.[9] Consequently, the capacity to efficiently prepare single enantiomers of an active pharmaceutical ingredient (API) or its intermediate is crucial for the pharmaceutical companies focused on discovery of new drug products.[10]

The techniques employed for the production of pure enantiomers can be divided into two approaches: a 'chiral approach' (chiral pool,[11] use of chiral auxiliaries,[12] asymmetric catalysis,[13] deracemization[14]) and a 'racemic approach' (chiral chromatography,[15] kinetic resolution,[16] diastereoisomeric salt formation,[17] cocrystallization,[18] preferential crystallization[19]). The former is based on the synthesis of enantiopure products, whereas the latter relies on the separation of mixtures of enantiomers in a process called 'chiral resolution'.[20] The main limitation of the 'chiral approach' is the fact that it is not always feasible or cost-effective. The 'racemic approach' requires that the enantiomers are resolved at the solid state. Whereas introduction of an enantiopure resolving agent is common, enantiomer separation without the introduction of such a chiral agent occurs in less than 10% of cases.[21]

Crystal engineering[22] approaches can be employed to increase the degree of control on the possibility for a compound to crystallize as conglomerate, with salt[23] or solvate[24] formation being, arguably, the most commonly used strategies. Cocrystallization[25] has emerged more recently as a viable tool to transform racemic compounds into conglomerates.[26]

[a] *F. Grepioni, D. Braga*
University of Bologna,
Department of Chemistry G. Ciamician,
Via F. Selmi 2, Bologna, Italy
E-mail: dario.braga@unibo.it
[b] *O. Shemchuk, T. Leyssens*
Institute Of Condensed Matter and Nanosciences,
UCLouvain, 1 Place Louis Pasteur,
B-1348 Louvain-la-Neuve, Belgium

In this topical review we describe a novel approach to chiral resolution in the solid state via cocrystallization of a racemic compound with an achiral inorganic salt coformer, with formation of ionic cocrystals (ICCs[28]). In particular, we focus our attention on the influence of the cationic species on the resolution propensity. Each family of compounds will be described with a focus on the formation of racemic crystals or conglomerates, or both. Before proceeding it is useful to stress that, in the context of this discussion, the term ionic cocrystal is used in a broad sense, to encompass aggregates of neutral or zwitterionic organic molecules with inorganic salts, such as LiX, CaX_2 and MgX_2 (X = Cl, Br, I) as well as with metal complexes such as $ZnCl_2$, in spite of the different nature of metal-ligand interactions. Our interest is in comparing the results of the cocrystallization experiments in terms of topology and chiral preference.

2. Cocrystallization of L- and DL-Histidine with Lithium Halides

The cocrystals obtained by reacting the amino acids L- and DL-histidine and L- and DL-proline with lithium[33,35] and calcium[34] halides are model compounds of the effect of metal coordination on chiral selection.

Let us start with the ICCs of DL-histidine with lithium halides, that can be obtained by both liquid assisted grinding (LAG) and evaporation from undersaturated aqueous solutions.

As shown in Table 1, cocrystallization of L- and DL-histidine with LiX leads to formation of the corresponding hydrated ICCs. All crystals share a common feature: the lithium cations are tetrahedrally coordinated by three histidine and one water molecules (Figure 1a). Each of the three histidine molecules interacts, in turn, with three Li^+ cations, and the main crystalline feature is an infinite chain of tetrahedra sharing vertices (Figure 1b). The halide anions are situated between the layers formed by L-histidine·Li^+ and D-histidine·Li^+ chains (Figure 1c).

Cocrystallization of the racemic amino acid with lithium chloride and bromide results in the isomorphous DL-His·LiCl · $1.5H_2O$ and DL-His·LiBr · $1.5H_2O$ (Figure 2), crystallizing in the centrosymmetric space group C2/c. Despite the fact that enantiopure L-His·LiCl·H_2O and L-His·LiBr·H_2O crystallize in the non-centrosymmetric space group $P2_12_12_1$, their crystal packings are extremely similar to those observed for the racemic ICCs. The most intriguing aspect is the complexation of the racemic amino acid to lithium cations: each Li^+ is selectively coordinated by amino acids of the same handedness, forming infinite chains of L-histidine·Li^+ and D-histidine·Li^+ (Figure 2). These chains are the same as those observed in the enantiopure ICCs. For all these reasons the racemic ICCs can be considered as "cocrystals" of L-His·LiCl/Br·H_2O and D-His·LiCl/Br·H_2O.

Taking up from the observation of this peculiar feature it is reasonable to wonder whether the limit of this separation could

Dr. Oleksii Shemchuk is a postdoctoral researcher at the University of Louvain-la-Neuve. He earned a PhD in Chemistry working in the Molecular Crystal Engineering group at the University of Bologna under the supervision of Prof. Grepioni. His current research interests are in the field of multiple crystal forms, molecular and ionic cocrystals, chirality and solid solutions.

Prof. Fabrizia Grepioni is full professor of Inorganic Chemistry at the University of Bologna. Past experiences include two years of R&D in the industry, a PhD in Chemistry, six years as associate professor at the University of Sassari. She is co-author of about 400 publications on solid-state chemistry and crystal engineering. Her current research activity is in the field of molecular crystal engineering (polymorphism, solid solutions, organic and inorganic cocrystals), with a special focus on systems of agrochemical and environmental interest.

Prof. Tom Leyssens is professor of Physical Chemistry at the University of Louvain-la-Neuve. Prior to joining university, he spent three years in pharmaceutical industry focusing on crystallization process development. His current research focuses on multi-component crystals of pharmaceutical compounds, their use in formulation as well as the development of novel solution-based applications of these systems such as resolution and purification. He co-authored about 100 publications, and acts as a consultant for multiple agrochemical and pharmaceutical companies.

Prof. Dario Braga is full professor of Chemistry. He is author or co-author of about 500 publications on solid-state chemistry and crystal engineering. His current interests are in the study of molecular and ionic cocrystals, solid solutions, polymorphs and hydrates. He was the first Scientific Editor of CrystEngComm. In 2005, together with his group, he founded the spinoff company PolyCrystalLine spa. He is Director of the Institute of Advanced Study of the University of Bologna. He is recipient of several awards, including the Nasini medal from the Inorganic Chemistry Division of the Italian Chemical Society and the Mammi medal from the Italian Crystallographic Association.

Table 1. Cocrystallization products mentioned in this review article for the reaction of racemic amino acids/APIs and metal salts.

Compound	LiX	$CaCl_2$, $MgCl_2$	$ZnCl_2$
DL-alanine	DL-Ala·LiCl·H_2O[29]	–	DL-Ala_2·$ZnCl_2$[30]
DL-valine	D-/L-Val·LiCl·H_2O[29]	–	DL-Val_2·$ZnCl_2$[31]
	DL-Val·LiCl·H_2O[29]		
DL-leucine	L-Leu·LiCl·H_2O[29]	–	–
	DL-Leu·LiCl·1.5H_2O[29]		
DL-isoleucine	D-/L-Ile·LiCl·H_2O[29]	–	DL-Ile_2·$ZnCl_2$[32]
DL-histidine	DL-His·LiBr·1.5H_2O[33]	DL-His_2·$CaCl_2$·3H_2O[34]	–
	DL-His·LiCl·H_2O	DL-His_2·$CaBr_2$·4H_2O[34]	
	D-/L-His·LiI·1.5H_2O[33]	DL-His_2·CaI_2 ·4H_2O[34]	
DL-proline	DL-Pro·LiCl·H_2O[35]	–	DL-Pro_2·$ZnCl_2$[36]
	D-/L-Pro·LiCl·H_2O[35]		DL-Pro_2·$ZnCl_2$[32]
	D-/L-Pro·LiBr·H_2O		
	DL-Pro·LiI·H_2O[35]		
	D-/L-Pro·LiCl[35]		
	DL-Pro·LiBr		
	DL-Pro·LiI[35]		
DL-serine	–	–	DL-Ser_2·$ZnCl_2$[32]
DL-threonine	–	–	DL-Thr_2·$ZnCl_2$·Thr[32]
DL-asparagine	–	–	DL-Asn_2·$ZnCl_2$[32]
DL-tyrosine	–	–	DL-Tyr·$ZnCl_2$[32]
DL-glutamic acid	–	–	DL-Glu_2·$ZnCl_2$[37]
RS-etiracetam	–	*RS*-ETI·$CaCl_2$·2H_2O[38]	*RS*-ETI_2·$ZnCl_2$[39]
		RS-ETI·$MgCl_2$·2H_2O[38]	*R-/S*-ETI·$ZnCl_2$[39]
RS-oxiracetam	–	*RS*-OXI_2·$CaCl_2$[40]	–
		R-/S-OXI·$MgCl_2$·5H_2O[40]	

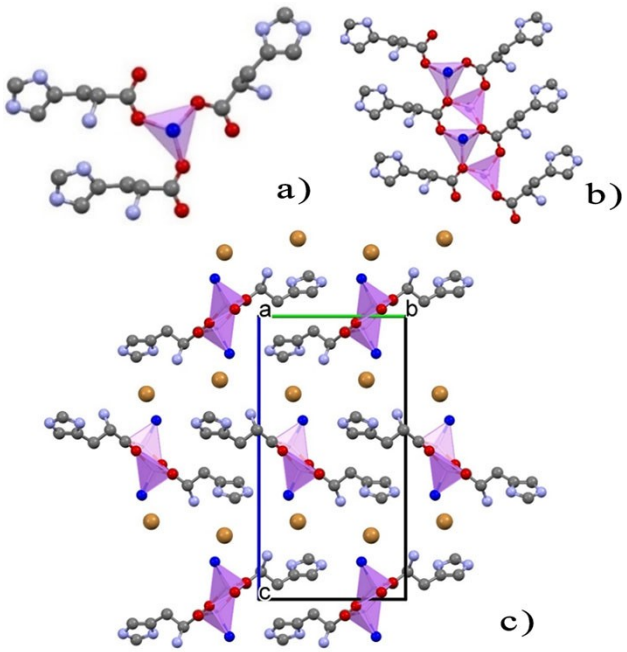

Figure 1. L-His·LiBr·H_2O (CSD refcode AZIPOQ[33]). (a) Tetrahedral coordination around the Li^+ cation; (b) portion of the infinite chain of lithium coordination tetrahedra; (c) crystal packing. Water oxygens in blue; Li^+ coordination polyhedra in lilac; bromide ions in brown; hydrogen atoms omitted for clarity.

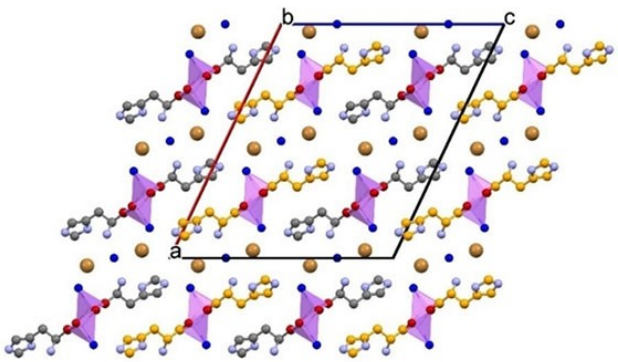

Figure 2. Crystal packing of DL-His·LiBr·1.5H_2O (CSD refcode AZIPIK[33]). Water oxygens in blue; grey and orange spheres for carbons ETI_2·$CaCl_2$·2H_2O refer to histidine molecules with opposite chirality; Li^+ coordination polyhedra in lilac; bromide ions in brown; Hydrogen atoms omitted for clarity.

be conglomerate formation. This is indeed observed when L- and DL-histidine are reacted with lithium iodide (Scheme 1): while the enantiopure ICC, L-His·LiI · 1.5H_2O is *quasi*-isostructural with L-His·LiCl·H_2O and L-His·LiBr·H_2O, cocrystallization of the racemic amino acid with LiI leads to chiral resolution, in the solid state, with formation of the conglomerate L-His·LiI · 1.5H_2O/D-His·LiI · 1.5H_2O.

Israel Journal of Chemistry

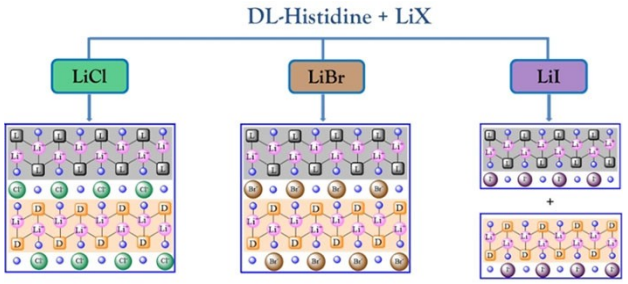

Scheme 1. Cocrystallization of DL-histidine with lithium halides. "L" and "D" stays for L- and D-histidine respectively; blue spheres represent water oxygens.

3. Cocrystallization of L- and DL-Histidine with Calcium Halides

Cocrystallization of L-histidine with calcium halides can also be performed via LAG and by evaporation of undersaturated solutions.[34] Importantly, contrary to what observed with LiX, cocrystallization of DL-histidine with calcium halides does not result in the formation of homochiral patterns. In all cases ribbon-like structures containing a central Ca^{2+} cation and homochiral strains on each side of this cation are formed (see figure 3). The calcium ions are hexa-coordinated through six oxygen atoms: two of L-histidine, two of D-histidine and two of water molecules.

It appears that in the ICCs with Ca^{2+} cations no chiral preference is observed, very likely because the octahedral coordination is compatible with the aggregation of amino acids of opposite handedness around an inversion centre, while the non-centrosymmetric nature of tetrahedral geometry around the small Li^+ cation appears to be less favourable for the aggregation of amino acids of the same chirality.

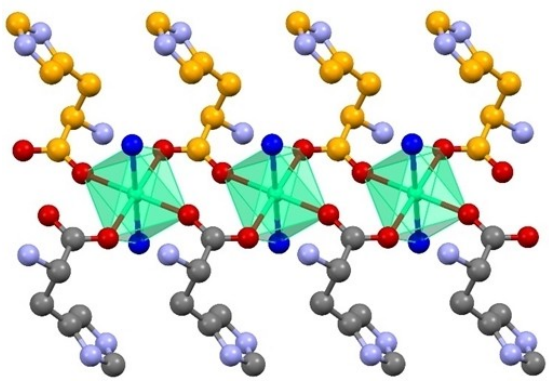

Figure 3. A ribbon of histidine bridged calcium cations in crystalline $(DL\text{-}His)_2 \cdot CaBr_2 \cdot 4H_2O$ (CSD refcode DEKSAQ[34]). Water oxygens in blue; grey and orange spheres for carbons refer to proline molecules with opposite chirality; Ca^{2+} coordination polyhedra in green; H atoms omitted for clarity.

4. Cocrystallization of L- and DL-Proline with Lithium Halides

In order to test these preliminary assumptions, lithium halides were cocrystallized with L- and DL-acid proline. In spite of the chemical and structural difference between the two amino acids, the outcome of the cocrystallization is very similar: complexation of Li^+ by proline appears to favours molecules of the same chirality. This feature is retained in both racemate and conglomerate crystals as well as in the respective dehydration products. As a matter of fact, the behaviour of histidine and proline upon reaction with LiX is very similar but not identical (compare schemes 1 and 2).

However, a remarkable difference is shown in the cases of the ICCs with LiCl. While DL-histidine forms the racemic crystal with distinct enantiopure chains as shown above, the ICC with DL-proline yields both a racemic crystal and a conglomerate of identical chemical compositions (see Scheme 2).[31]

4.1. Dehydration of the ICCs of DL-Proline

Upon dehydration all ICCs discussed so far remain crystalline. The structural motif of 1D-chains observed in the hydrated forms is maintained in the anhydrous ICC, although the halide anions have now replaced the water molecules in the tetrahedral coordination sphere around the lithium cations (Figure 4 in the case of L-Pro-LiI).

A clear-cut homochiral preference of lithium cations is maintained in all the anhydrous ICCs, with Li^+ being selectively bound to molecules of single handedness thus forming infinite "enantiopure" $(L\text{-}Pro \cdot LiI)_n/(D\text{-}Pro \cdot LiI)_n$ chains (Figure 5).

The outcomes of dehydration/rehydration processes, as well as the structural relationship between pairs of crystals, are summarized in Scheme 3.

Dehydration of both $D\text{-}Pro \cdot LiCl \cdot H_2O/L\text{-}Pro \cdot LiCl \cdot H_2O$ and $DL\text{-}Pro \cdot LiCl \cdot H_2O$ results in the formation of the conglomerate L-Pro·LiCl/D-Pro·LiCl. The rehydration, in turn, invariably yields the racemic form. Dehydration of the

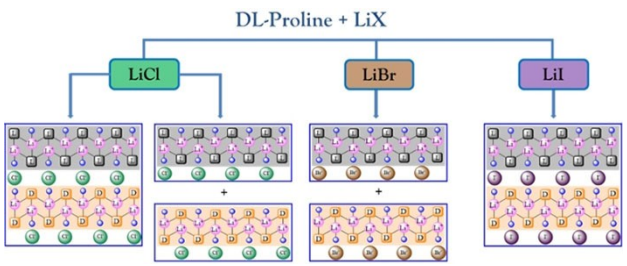

Scheme 2. Cocrystallization of DL-proline with lithium halides. "L" and "D" stay for L- and D-proline respectively; blue spheres represent water oxygens.

Israel Journal of Chemistry

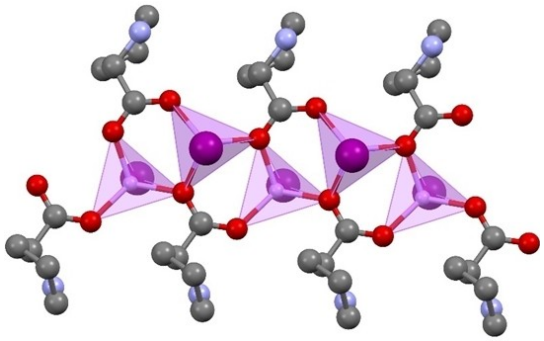

Figure 4. The 1D-chain structural motif observed in the hydrated forms is maintained in anhydrous L-Pro·LiI (CSD refcode MISKAD[35]), but the halide anions replace the water molecules in the tetrahedral coordination sphere around the lithium cations. Li^+ coordination polyhedra in lilac; iodide ions in purple; H atoms omitted for clarity.

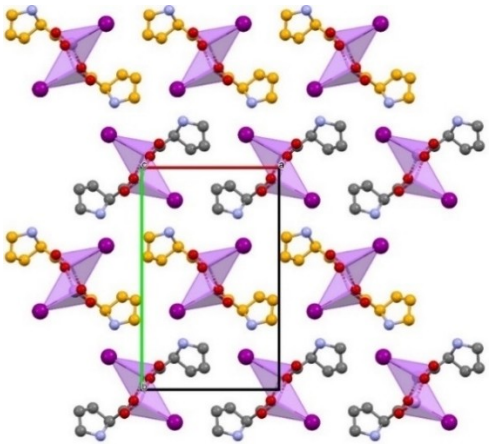

Figure 5. The crystal packing arrangement of DL-Pro·LiI (CSD refcode MISKEH[35]). Grey and orange spheres for carbons refer to proline molecules with opposite chirality; Li^+ coordination polyhedra in lilac; iodide ions in purple; H atoms omitted for clarity.

conglomerate L-Pro·LiBr·H_2O /D-Pro·LiBr·H_2O, on the other hand, yields the racemate DL-Pro·LiBr, which converts back to the conglomerate upon rehydration. Finally, the racemate DL-Pro·LiI·H_2O maintains its racemate nature upon dehydration (Figure 5) and subsequent rehydration. The dehydration/hydration processes in Scheme 3 are also indicative of the small difference in lattice energy between racemic and conglomerate structures, with conglomerates generally thermodynamically penalized due to limited packing arrangements to accommodate the chiral molecules.[41] As a matter of fact, the packing coefficients of all the ICCs discussed in this paper differ only slightly on passing from enantiopure to racemic cocrystals.[35]

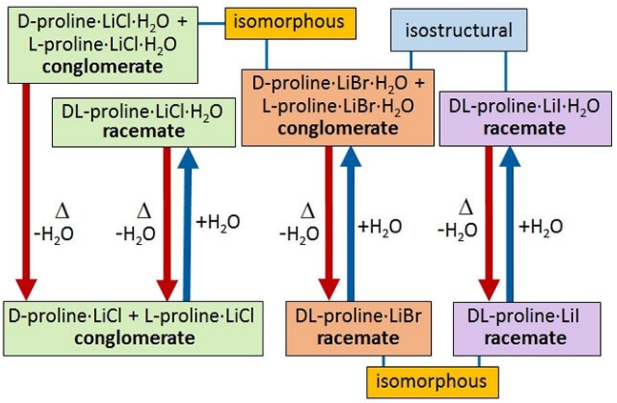

Scheme 3. Dehydration/rehydration processes involving all the hydrated ICCs containing both L- and D-proline enantiomers; structural relationships between isomorphous pairs indicated in yellow. Reproduced from Ref. [35] with permission from Wiley.

5. Cocrystallization of DL-Alanine, DL-Valine, DL-Leucine and DL-Isoleucine with LiCl

In order to further test the transferability to other systems of the findings discussed above, a whole series of hydrophobic amino acids has also been cocrystallized with LiCl (see Scheme 4).[29] While the cocrystallization of LiCl with DL-alanine does not lead to chiral resolution, in the case of DL-valine and DL-leucine a solvent dependent formation is observed of metastable conglomerates, that transform over time into stable racemic products. Cocrystallization of DL-isoleucine (commercially available as a solid solution of D- and L-isoleucine and of D- and L-alloisoleucine) with LiCl also results in a complex mixture of metastable products, that transforms over time into stable conglomerates, as shown in Scheme 4.

In the cases of DL-valine, DL-leucine and DL-isoleucine the racemic *versus* conglomerate nature of the ICCs prepared

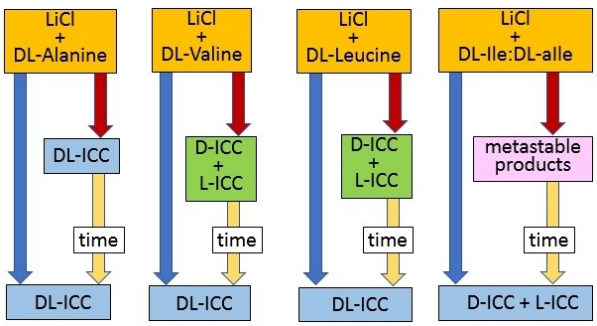

Scheme 4. Reactivity of the four zwitterionic DL-amino acids with LiCl in the presence of water (blue arrows) or methanol (red arrows), and conglomerate (D-ICC + L-ICC) vs. racemic compounds (DL-ICC) formation. Commercial DL-isoleucine, indicated here as DL-Ile:DL-alle, is a 1:1:1:1 solid solution of L-Ile, D-Ile, L-alle and D-alle.

by LAG depends on whether methanol or water is used. The crystallization from aqueous solutions yields different products from those obtained by ball milling with a few drops of methanol. As in the cases of the ICCs of DL-histidine and DL-proline with lithium halides discussed above, the homochiral preference of lithium cations is observed.

6. Cocrystallization of Alanine, Valine, Proline, Isoleucine, Serine, Threonine, Asparagine and Tyrosine with $ZnCl_2$

To understand whether the phenomenon of lithium homochiral preference is an intrinsic property of the Li^+ cation or does indeed depend on the tetrahedral complexation geometry, the most viable route is the use of another metal cation, such as Zn^{2+}, known to favour tetrahedral coordination. To this end, a series of amino acids was cocrystallized with zinc chloride.[32] An analysis of the crystal structures of *DL*-ala$_2\cdot ZnCl_2$,[30] *DL*-val$_2\cdot ZnCl_2$[31] and *DL*-pro$_2\cdot ZnCl_2$,[36] previously investigated by others, confirmed that in all cases the Zn^{2+} cations were selectively coordinated by amino acids of the same handedness. When the analysis is extended to the cocrystallization of $ZnCl_2$ with the D,L-amino acids alanine, valine, proline, isoleucine, serine, threonine, asparagine and tyrosine, the overall picture that emerges is that, when the stoichiometric ratio amino acid:metal cation is 2 : 1, the Zn^{2+} centre favours complexation with two molecules of amino acid of the same handedness (this is the case of DL-Ala$_2\cdot ZnCl_2$, DL-Val$_2\cdot ZnCl_2$, DL-Pro$_2\cdot ZnCl_2$, DL-Ile$_2\cdot ZnCl_2$, and DL-Ser$_2\cdot ZnCl_2$[32]). The crystal structure of DL-Ser$_2\cdot ZnCl_2$ is shown as an example in Figure 6. Analogous behaviour is shown by DL-Glu$_2\cdot ZnCl_2$.[37] Since all complexes crystallize in centrosymmetric space groups, the homochiral complexation implies that both D-AA$_2\cdot ZnCl_2$ and L-AA$_2\cdot ZnCl_2$ are present in 1 : 1 ratio within the same crystal. However, contrary to the lithium halide cases,[29,33,35] no conglomerates are observed.

Interestingly, in a first attempt of reproducing the synthesis of the previously reported DL-Pro$_2\cdot ZnCl_2$, which shows homochiral coordination around Zn,[36] an heterochiral complex is obtained (see Figure 7). The homochiral complex could, however, be obtained, starting from the reagents, in a slurry experiment, suggesting a higher stability for this form with respect to the heterochiral one. All subsequent attempts to reproduce the heterochiral DL-Pro$_2\cdot ZnCl_2$ complex, however, were unsuccessful, and the homochiral complex is now invariably produced.

Another exception to the "homochiral coordination rule" is represented by the peculiar cocrystal of DL-threonine with $ZnCl_2$, DL-thr$_2\cdot ZnCl_2\cdot$thr, shown in Figure 8.

An alternative structure is shown by the 1 : 1 cocrystals of asparagine and tyrosine with $ZnCl_2$. Figure 9 shows a 1D coordination polymer whereby the two amino acids act as bidentate divergent ligands. In these cases, the *D*- and *L*-amino acids alternate along the 1D polymer so that no chiral preference or segregation is observed.

7. Cocrystallization of Etiracetam with $ZnCl_2$

As mentioned in the Introduction, the possibility of attaining chiral selection upon simple coordination may have important consequences in the pharmaceutical field. For this reason the interaction of the antiepileptic drug levetiracetam (enantiopure

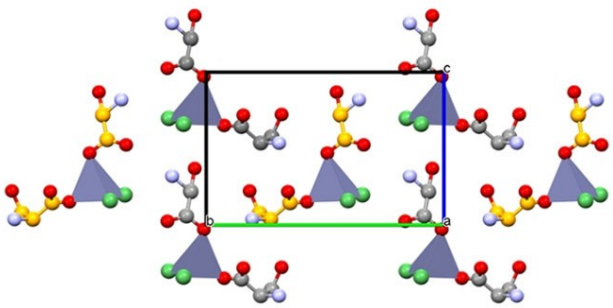

Figure 6. The homochiral complexes in crystalline *DL*-ser$_2\cdot ZnCl_2$ (view in the *bc*-plane). D-serine carbon atoms in orange. H atoms omitted for clarity. Grey and orange spheres for carbons refer to serine molecules with opposite chirality; Zn^{2+} coordination polyhedra in blue-grey; chloride ions in lime green; Reproduced from Ref. [32] with permission from the Royal Society of Chemistry.

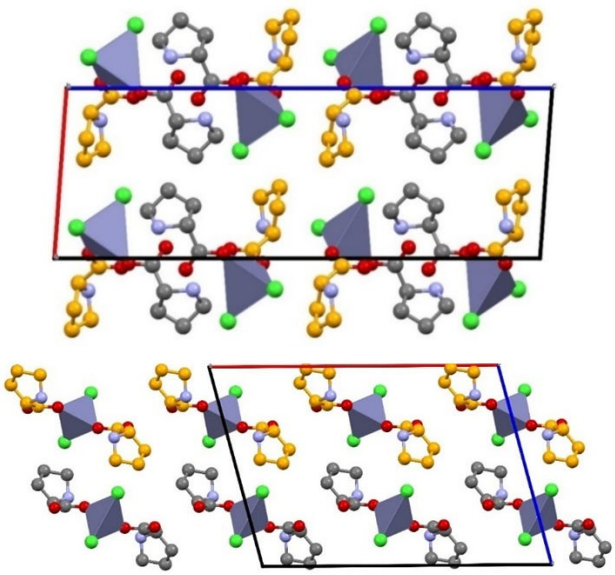

Figure 7. Comparison between crystal packings for homochiral (top) and heterochiral (bottom) DL-pro$_2\cdot ZnCl_2$. Grey and orange spheres for carbons refer to proline molecules with opposite chirality; Zn^{2+} coordination polyhedra in blue-grey; chloride ions in lime green; H atoms omitted for clarity. Reproduced from Ref. [32] with permission from the Royal Society of Chemistry.

Israel Journal of Chemistry

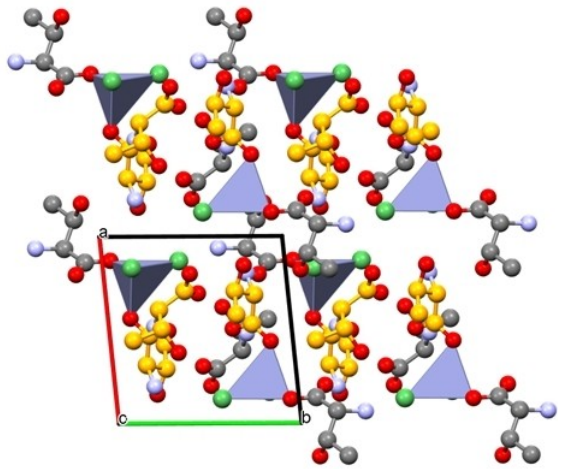

Figure 8. View in the crystallographic *ab*-plane of crystalline DL-thr$_2$·ZnCl$_2$·thr, containing racemic threonine in addition to the heterochiral zinc(II) complexes. Grey and orange spheres for carbons refer to threonine molecules with opposite chirality; Zn^{2+} coordination polyhedra in blue-grey; chloride ions in lime green; H atoms omitted for clarity. Reproduced from Ref. [32] with permission from the Royal Society of Chemistry.

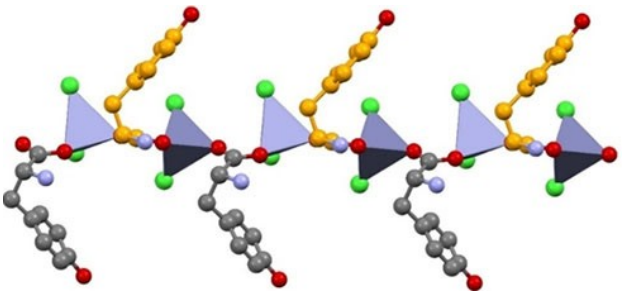

Figure 9. *catena*-[(μ_2-*DL*-tyrosine)ZnCl$_2$]. Note how both oxygens of tyrosine carboxylate participate in coordination to the Zn^{2+} cations. Grey and orange spheres for carbons refer to tyrosine with opposite chirality; Zn^{2+} coordination polyhedra in blue-grey; chloride ions in lime green; Reproduced from Ref. [32] with permission from the Royal Society of Chemistry.

S-etiracetam) and its racemic intermediate *RS*-etiracetam (Scheme 5) with ZnCl$_2$ was investigated.[39]

Reaction of both levetiracetam (*S*-ETI) and etiracetam (*RS*-ETI) with ZnCl$_2$ results in the formation of anhydrous complexes – *S*-ETI·ZnCl$_2$ (Figure 10) and Eti$_2$·ZnCl$_2$ (Figure 11), respectively. A 1 : 1 *S*-ETI:Zn^{2+} stoichiometric ratio is observed with both Zn^{2+} cations, tetrahedrally coordinated by two APIs, which act as bridges, via the pyrrolidone and the amido groups, between consecutive zinc cations, thus forming infinite zig-zag chains.

The complexation of racemic etiracetam with ZnCl$_2$ results in the crystalline compound *RS*-ETI$_2$·ZnCl$_2$ (Figure 11). Like for most of the obtained complexes of ZnCl$_2$ with amino acids mentioned above, a 2 : 1 stoichiometry is also observed (*RS*-

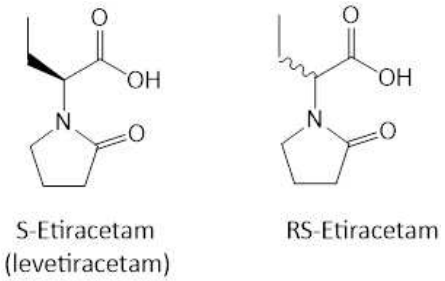

Scheme 5. Chemical structures of Etiracetam (*RS*-ETI) and Levetiracetam (*S*-ETI, the biologically active enantiomer).

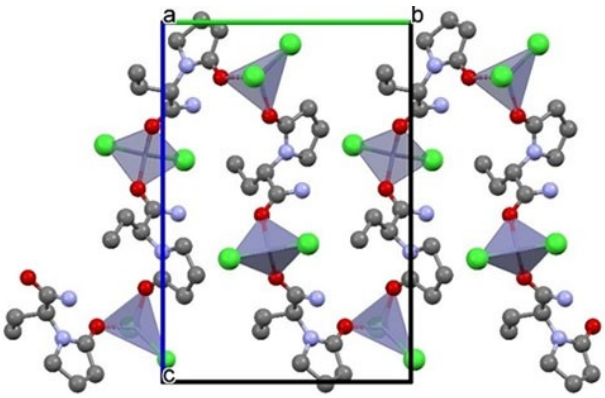

Figure 10. The crystal packing of *S*-ETI·ZnCl$_2$ (CSD refcode KIJSII[39]): infinite zig-zag chain formed by ZnCl$_2$ units bridged by *S*-ETI molecules. Zn^{2+} coordination polyhedra in blue-grey Chloride ions in lime green. H atoms omitted for clarity.

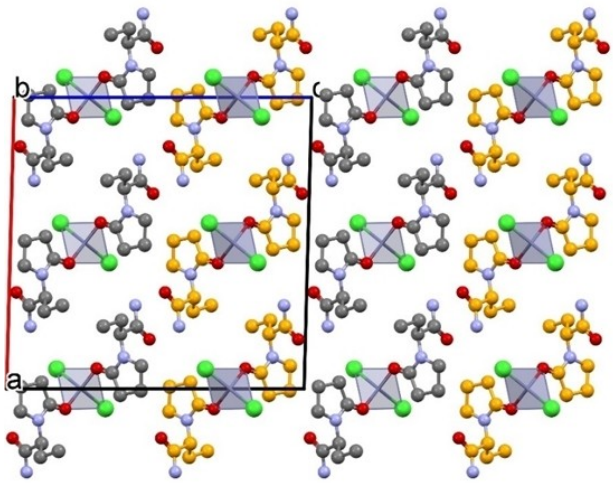

Figure 11. Crystal packing of Eti$_2$·ZnCl$_2$ (CSD refcode KIJSEE[39]). Grey and orange spheres for carbons refer to racetams with opposite chirality; Zn^{2+} coordination polyhedra in blue-grey; chloride ions in lime green; H atoms omitted for clarity.

$ETI_2{\cdot}ZnCl_2$), as only the oxygen of pyrrolidone is bound to Zn^{2+}, resulting in a 0D complex. It is worth pointing out that the Zn^{2+} cations selectively bind to molecules of one chirality, forming distinct layers of *R*-$ETI_2{\cdot}ZnCl_2$ and of *S*-$ETI_2{\cdot}ZnCl_2$ in the overall racemic compound.

Interestingly, increasing the amount of $ZnCl_2$ with respect to *RS*-etiracetam (from 2 : 1 to 1 : 1 ratio) leads to disruption of the racemic compound, with the formation of a stable conglomerate *R*-ETI·$ZnCl_2$ + *S*-ETI·$ZnCl_2$ (see Scheme 6). In turn, adding an equivalent of etiracetam to the conglomerate leads to the formation of the racemic compound, offering a stoichiometric switch between a stable racemic compound and a stable conglomerate.

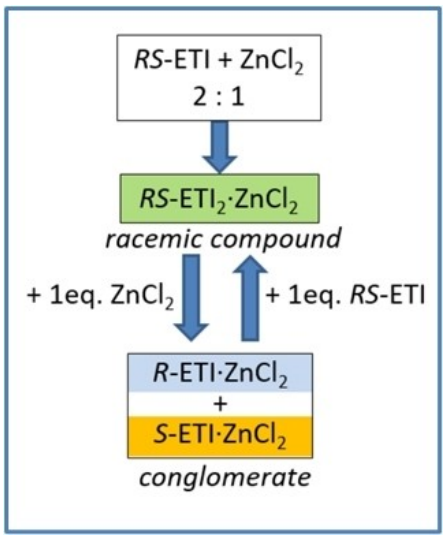

Scheme 6. Graphic representation of the *RS*-ETI:$ZnCl_2$ system in the solid-state, and the role of stoichiometry in the racemic compound/conglomerate switch mechanism. Reproduced from Ref. [39] with permission from the Royal Society of Chemistry.

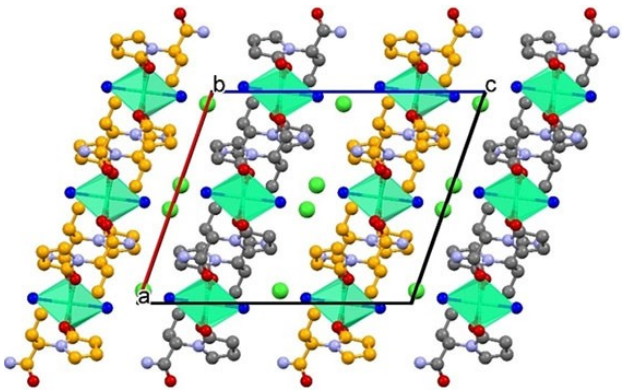

Figure 12. $ETI_2{\cdot}CaCl_2{\cdot}2H_2O$ (CSD refcode VOCGAY[38]): parallel 2D-layers projected down the *b*-axis. Water oxygens in blue; grey and orange spheres for carbons $ETI_2{\cdot}CaCl_2{\cdot}2H_2O$ refer to racetams with opposite chirality; Ca^{2+} coordination polyhedra in green; chloride ions in lime; H_{CH} atoms omitted for clarity.

8. Cocrystallization of Etiracetam and Oxiracetam with $CaCl_2$ and $MgCl_2$

When cocrystallization of enantiopure and racemic etiracetam with calcium and magnesium chlorides (Scheme 5) is investigated, a complex solid-state landscape of ionic cocrystals is observed. Among others, isomorphous ICCs are observed for $ETI_2{\cdot}CaCl_2{\cdot}2H_2O$ and $ETI_2{\cdot}MgCl_2{\cdot}2H_2O$, characterized by an octahedral coordination around the metal cation (Figure 12), comprising the oxygens of four different molecules of etiracetam and two water molecules. Each etiracetam, in turn, interacts with two metal cations, resulting in a 2D-layered structure. Intriguingly, the formation of enantiospecific complexes is observed, resulting into quasi-isostructural racemic and enantiopure materials. This packing choice is reminiscent of what is systematically observed in the ICCs of the amino acids with lithium halides, but rules out the necessity for a tetrahedral arrangement to induce homochiral coordination.[29,33,35]

When RS-oxiracetam and S-oxiracetam (Scheme 7) are cocrystallized with $MgCl_2$[40] spontaneous chiral resolution of RS-oxiracetam, with formation of a stable *S*-OXI·$MgCl_2 \cdot 5H_2O$/*R*-OXI·$MgCl_2 \cdot 5H_2O$ conglomerate, is observed (Figure 13), irrespective of the cocrystallization methods applied, i.e. LAG, evaporation from undersaturated solution and slurry mediated transformation. The conglomerate *S*-OXI·$MgCl_2 \cdot 5H_2O$/*R*-OXI·$MgCl_2 \cdot 5H_2O$, is isostructural with the cocrystal obtained when enantiopure S-oxiracetam is used.

9. Summary and Outlook

In this article we have reviewed the results obtained in a series of investigations of the preference for the formation of racemic or conglomerate crystalline materials upon reaction of racemic mixtures of chiral molecules with alkali and alkaline earth metal halides and with zinc chloride. We have compared the products obtained with the racemic mixtures with those obtained with the enantiopure systems.

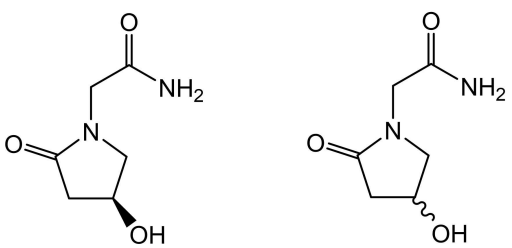

Scheme 7. Chemical structure of enantiopure (left) and racemic (right) oxiracetam.

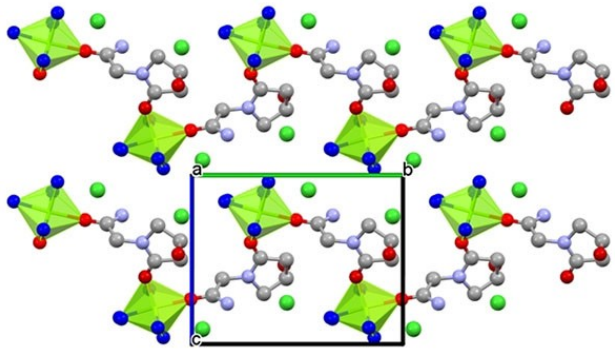

Figure 13. The crystal packing of S-OXI·$MgCl_2$·$5H_2O$, showing the 1-D zig-zag chains extending parallel to the crystallographic b-axis. Water oxygens in blue; Mg^{2+} coordination polyhedra and chloride ions in lime green; H atoms omitted for clarity.

The principal objective was that of verifying the initial, rather serendipitous and intriguing observation that the racemic amino acid DL-proline, when reacted with LiX (X = Cl, Br, I), forms ionic co-crystals containing enantiopure chains of tetrahedrally coordinated Li^+ cations, irrespective of the racemic or conglomerate nature of the products. The enantiopure chains are related by centrosymmetry in the racemic crystals.

Indeed, we have found that an analogous behaviour is observed with other chiral molecules also available as enantiopure and racemic mixtures. When the ionic cocrystal involves the Li^+ and the Zn^{2+} cations, that favour tetrahedral coordination, complexation leads to chiral selection, with formation of racemic crystals containing enantiopure complexes or chains and formation of conglomerates. When both situations are observed, as in the case of D-/L-Pro·LiCl·H_2O, the racemic and the conglomerate crystal contain exactly the same type of arrangement. On the contrary, when complexation involves cations such as Ca^{2+} and Mg^{2+} that favour octahedral coordination, chiral selection is not observed in the majority of cases.

Further work is under way to establish to what extent these behaviours can be generalized to other classes of racemic organic compounds and/or to other metal type and coordination modes.

Acknowledgements

The *"FSR Incoming Post-doctoral Fellowship"* is acknowledged for financial support of OS. The University of Bologna is acknowledged for financial support. Open Access Funding provided by Universita di Bologna within the CRUI-CARE Agreement.

References

[1] W. A. Bonner, *Orig Life Evol Biosph* **1995**, *25*, 175–190.
[2] N. M. Maier, P. Franco, W. Lindner, *J. Chromatogr. A* **2001**, *906*, 3–33.
[3] H. Y. Aboul-Enein, I. W. Wainer, *The impact of stereochemistry on drug development and use, Vol. 142*, Wiley-Interscience, **1997**.
[4] E. Francotte, W. Lindner, *Chirality in drug research, Vol. 33*, Wiley-VCH Weinheim, **2006**.
[5] R. Xie, L. Y. Chu, J. G. Deng, *Chem. Soc. Rev.* **2008**, *37*, 1243–1263.
[6] W. Lenz, *Teratology* **1988**, *38*, 203–215.
[7] H. Caner, E. Groner, L. Levy, I. Agranat, *Drug Discovery Today* **2004**, *9*, 105–110.
[8] E. J. Ariens, *Eur. J. Clin. Pharmacol.* **1984**, *26*, 663–668.
[9] US Food and Drug administration (2014) Development of Stereoisomeric Drugs, **2014**, https://www.fda.gov/drugs/.
[10] H. Leek, L. Thunberg, A. C. Jonson, K. Ohlen, M. Klarqvist, *Drug Discovery Today* **2017**, *22*, 133–139.
[11] H. U. Blaser, *Chem. Rev.* **1992**, *92*, 935–952.
[12] D. J. Ager, I. Prakash, D. R. Schaad, *Chem. Rev.* **1996**, *96*, 835–876.
[13] R. Noyori, *Angew. Chem. Int. Ed.* **2002**, *41*, 2008–2022; *Angew. Chem.* **2002**, *114*, 2108–2123.
[14] a) C. Viedma, *Phys. Rev. Lett.* **2005**, *94*, 065504; b) W. L. Noorduin, T. Izumi, A. Millemaggi, M. Leeman, H. Meekes, W. J. Van Enckevort, R. M. Kellogg, B. Kaptein, E. Vlieg, D. G. Blackmond, *J. Am. Chem. Soc.* **2008**, *130*, 1158–1159; c) W. L. Noorduin, W. J. van Enckevort, H. Meekes, B. Kaptein, R. M. Kellogg, J. C. Tully, J. M. McBride, E. Vlieg, *Angew. Chem. Int. Ed.* **2010**, *49*, 8435–8438; *Angew. Chem.* **2010**, *122*, 8613–8616; d) W. W. Li, L. Spix, S. C. A. de Reus, H. Meekes, H. J. M. Kramer, E. Vlieg, J. H. ter Horst, *Cryst. Growth Des.* **2016**, *16*, 5563–5570; e) C. Xiouras, J. H. Ter Horst, T. Van Gerven, G. D. Stefanidis, *Cryst. Growth Des.* **2017**, *17*, 4965–4976.
[15] T. E. Beesley, R. P. Scott, *Chiral chromatography*, John Wiley & Sons, **1999**.
[16] C. S. Chen, Y. Fujimoto, G. Girdaukas, C. J. Sih, *J. Am. Chem. Soc.* **1982**, *104*, 7294–7299.
[17] D. Kozma, *CRC handbook of optical resolutions via diastereomeric salt formation*, Crc Press, **2001**.
[18] a) G. R. Springuel, T. Leyssens, *Cryst. Growth Des.* **2012**, *12*, 3374–3378; b) B. Harmsen, T. Leyssens, *Cryst. Growth Des.* **2017**, *18*, 441–448.
[19] a) G. Coquerel, in *Novel optical resolution technologies*, Springer, **2006**, pp. 1–51; b) G. Levilain, G. Coquerel, *CrystEngComm* **2010**, *12*, 1983–1992.
[20] H. Lorenz, A. Seidel-Morgenstern, *Angew. Chem. Int. Ed. Engl.* **2014**, *53*, 1218–1250.
[21] a) S. Srisanga, J. H. ter Horst, *Cryst. Growth Des.* **2010**, *10*, 1808–1812; b) K. Sakai, N. Hirayama, R. Tamura, *Novel optical resolution technologies, Vol. 269*, Springer, **2007**; c) J. Jacques, A. Collet, S. Wilen, *Enantiomers, Racemates, and Resolutions*. John Wiley & Sons, **1981**; d) T. Rekis, *Acta Crystallogr.* **2020**, *B76*, 307–315.
[22] G. R. Desiraju, G. W. Parshall, *Mater. Sci. Monogr.* **1989**, *54*.
[23] W. W. Li, L. Spix, S. C. De Reus, H. Meekes, H. J. Kramer, E. Vlieg, J. H. ter Horst, *Cryst. Growth Des.* **2016**, *16*, 5563–5570.
[24] S. Wacharine-Antar, G. Levilain, V. Dupray, G. Coquerel, *Org. Process Res. Dev.* **2010**, *14*, 1358–1363.
[25] a) O. Almarsson, M. J. Zaworotko, *Chem. Commun.* **2004**, *0*, 1889–1896; b) C. B. Aakeröy, D. J. Salmon, *CrystEngComm*

2005, *7*, 439–448; c) A. Karagianni, M. Malamatari, K. Kachrimanis, *Pharmaceutica* **2018**, *10,* 18–47; d) I. Sathisaran, S. V. Dalvi, *Pharmaceutica* **2018**, *10*, 108–181; e) Z. X. Ng, D. Tan, W. L. Teo, F. Leon, X. Shi, Y. Sim, Y. Li, R. Ganguly, Y. Zhao, S. Mohamed, F. Garcia, *Angew. Chem. Int. Ed.* **2021**, *60*, 2–12; f) M. Solares-Briones, G. Coyote-Dotor, J. C. Páez-Franco, M. R. Zermeño-Ortega, C. M. de la O Contreras, D. Canseco-González, A. Avila-Sorrosa, D. Morales-Morales, J. M. Germán-Acacio, *Pharmaceutica* **2021**, *13*, 790–840.

[26] a) M. Guillot, J. de Meester, S. Huynen, L. Collard, K. Robeyns, O. Riant, T. Leyssens, *Angew. Chem. Int. Ed.* **2020**, *59*, 11303–11306; *Angew. Chem.* **2020**, *132*, 11399–11402; b) N. Blagden, M. de Matas, P. T. Gavan, P. York, *Adv. Drug Delivery Rev.* **2007**, *59*, 617–630; c) T. Friščić, W. Jones, *J. Pharm. Pharmacol.* **2010**, *62*, 1547–1559; d) C. C. Sun, *Expert Opin. Drug Delivery* **2013**, *10*, 201–213.

[27] a) L. C. Harfouche, C. Brandel, Y. Cartigny, S. Petit, G. Coquerel, *Chem. Eng. Technol.* **2020**, *43*, 1093–1098; b) X. Buol, C. Caro Garrido, K. Robeyns, N. Tumanov, L. Collard, J. Wouters, T. Leyssens, *Cryst. Growth Des.* **2020**, *20*, 7979–7988; c) C. Neurohr, M. Marchivie, S. Lecomte, Y. Cartigny, N. Couvrat, M. Sanselme, P. Subra-Paternault, *Cryst. Growth Des.* **2015**, *15*, 4616–4626; d) W. Li, M. de Groen, H. J. M. Kramer, R. de Gelder, P. Tinnemans, H. Meekes, J. H. ter Horst, *Cryst. Growth Des.* **2020**, *21*, 112–124; e) K. K. Sarmah, T. Rajbongshi, A. Bhuyan, R. Thakuria, *Chem. Commun.* **2019**, *55*, 10900–10903.

[28] D. Braga, F. Grepioni, L. Maini, S. Prosperi, R. Gobetto, M. R. Chierotti, *Chem. Commun.* **2010**, *46*, 7715–7717.

[29] O. Shemchuk, E. Spoletti, D. Braga, F. Grepioni, *Cryst. Growth Des.* **2021**, 21, 6, 3438–3448.

[30] M. Subha Nandhini, R. V. Krishnakumar, S. Natarajan, *Acta Crystallogr. Sect. E* **2002**, *58*, m127-m129.

[31] M. S. Nandhini, R. V. Krishnakumar, S. Natarajan, *Acta Crystallogr. Sect. E* **2001**, *57*, m498-m500.

[32] O. Shemchuk, F. Grepioni, D. Braga, *CrystEngComm* **2020**, *22*, 5613–5619.

[33] D. Braga, L. Degli Esposti, K. Rubini, O. Shemchuk, F. Grepioni, *Cryst. Growth Des.* **2016**, *16*, 7263–7270.

[34] O. Shemchuk, L. Degli Esposti, F. Grepioni, D. Braga, *CrystEngComm* **2017**, *19*, 6267–6273.

[35] a) O. Shemchuk, B. K. Tsenkova, D. Braga, M. T. Duarte, V. Andre, F. Grepioni, *Chem. Eur. J.* **2018**, *24*, 12564–12573; b) E. D'Oria, P. G. Karamertzanis, S. L. Price, *Cryst. Growth Des.* **2010**, *10*, 1749–1756.

[36] M. Lutz, R. Bakker, *Acta Crystallogr. Sect. C* **2003**, *59*, m18–20.

[37] O. Shemchuk, F. Grepioni, D. Braga, CCDC 2087822: Experimental Crystal Structure Determination. **2021**.

[38] L. Song, O. Shemchuk, K. Robeyns, D. Braga, F. Grepioni, T. Leyssens, *Cryst. Growth Des.* **2019**, *19*, 2446–2454.

[39] O. Shemchuk, L. Song, K. Robeyns, D. Braga, F. Grepioni, T. Leyssens, *Chem. Commun.* **2018**, *54*, 10890–10892.

[40] O. Shemchuk, L. Song, N. Tumanov, J. Wouters, D. Braga, F. Grepioni, T. Leyssens, *Cryst. Growth Des.* **2020**, *20*, 2602–2607.

[41] F. George, B. Norberg, K. Robeyns, J. Wouters, T. Leyssens, *Cryst. Growth Des.* **2016**, *16*, 5273–5282.

Manuscript received: June 9, 2021
Revised manuscript received: July 22, 2021
Version of record online: August 19, 2021

